POLARIZATION OF PHOTONS UNDER CONDITIONS OF INTERFERENCE BETWEEN THE PARAMETRIC RADIATION AND COHERENT BREMSSTRAHLUNG

S. V. Blazhevich, N. N. Nasonov, V. P. Petukhov, G. P. Pokhil, V. I. Sergienko, and V. A. Khablo

UDC 537.8

X rays emitted by relativistic electrons traversing a system of parallel atomic planes of a crystal are considered. The spectral, angular, and polarization characteristics of emitted photons are studied theoretically simultaneously for two coherent emission mechanisms, namely, the coherent bremsstrahlung and parametric X rays. Based on the results obtained, an optimal design of the experiment on studying the effect of interference of these emission mechanisms on the polarization of photons is calculated. The developed experimental facility is described.

INTRODUCTION

The complexity and the high expense of synchrotron accelerators that are now the main sources of quasi-monochromatic unidirectional x rays used for research and applied purposes stimulate a search for alternative methods of their generation. One of the most promising directions in this field is the study of parametric x rays (PXR) emitted by the relativistic electrons in crystals [1–3] that withstand electron beams with energies from one to two orders of magnitude lower compared to those obtained in synchrotron accelerators. The energy of PXR quanta increases as the angle defining the orientation of the electron momentum with respect to the reflecting crystallographic plane decreases (this circumstance allows the electron energy to be reduced). In this case, for orientation angles compared to the characteristic angle of relativistic particle emission $\gamma^{-1} = m/e$ (where m and e are the mass and energy of the emitting electron, respectively), the interference contribution of the coherent electron bremsstrahlung becomes significant (see theoretical grounding in [4] and experimental verification in [5]).

The present work is devoted to a detailed theoretical analysis of the above-described interference effect and to a design of the experiment which is being prepared now. Unlike [4], small orientation angles are used here, which allows the radiation properties to be described much better. In particular, the interference polarization characteristics of radiation that were not considered in [4] are analyzed here together with the effect of multiple scattering of the emitting electrons. The feasibility of application of the interference effect to increase the spectral and angular radiation density is also analyzed.

The optimal design of the experiment on the study of the polarization characteristics of the emitted photons is calculated under conditions of interference between the PXR and coherent bremsstrahlung, and the experimental facility which is being developed now is described.

1. RADIATION AMPLITUDE

Let us consider the structure of an electromagnetic field excited by a relativistic particle with charge q moving in a crystal. We proceed from the Maxwell equations

Laboratory of Radiation Physics at Belgorod State University; Scientific Research Institute of Atomic Physics at M. V. Lomonosov Moscow State University; P. N. Lebedev Institute of Physics.

$$(k^2-\omega^2)\boldsymbol{E}_{k\omega}-\boldsymbol{k}(\boldsymbol{k},\boldsymbol{E}_{k\omega})=4\pi i\omega\left(\boldsymbol{j}_{k\omega}+\frac{q}{(2\pi)^4}\int dt\,\boldsymbol{v}_q e^{i\omega t-i\boldsymbol{kr}_q}\right). \tag{1}$$

Here $\boldsymbol{E}_{k\omega}$ is the Fourier transform of the electric field strength, $\boldsymbol{r}_q(t)$ specifies the particle trajectory, $\boldsymbol{v}_q = d\boldsymbol{r}_q/dt$, and $\boldsymbol{j}_{k\omega}$ is the Fourier transform of the electron current density induced in the medium by the particle field.

In the x-ray range of energy of emitted quanta of interest to us,

$$I \ll \omega \ll m, \tag{2}$$

where I is the average atomic ionization potential of the crystal and m is the electron mass, we can neglect the energy of electron binding in the atom and the Compton change of ω in the process of scattering of the fast-particle field on the atom. In this case, the electron current density operator in the medium is determined by the expression [6]

$$\hat{\boldsymbol{j}}=-\frac{e^2}{m}\boldsymbol{A}(\boldsymbol{r},t)\hat{n}\,,\qquad \hat{n}=\sum_{\alpha}\sum_{\beta=1}^{Z}\delta(\boldsymbol{r}-\boldsymbol{r}_\alpha-\boldsymbol{r}_{\alpha\beta})\,, \tag{3}$$

widely used in the theory of x-ray scattering in a substance, where $\boldsymbol{A}$ is the vector potential of the field, $\boldsymbol{r}_\alpha$ specifies coordinates of atomic nuclei, and $\boldsymbol{r}_{\alpha\beta}$ specifies coordinates of atomic electrons.

From Eqs. (1) and (3), we obtain the equation

$$(k^2-\omega^2)\boldsymbol{E}_{k\omega}-\boldsymbol{k}(\boldsymbol{k},\boldsymbol{E}_{\pi\omega})+\int dk'\,G(\boldsymbol{k}'-\boldsymbol{k})\boldsymbol{E}_{\pi'\omega}=\frac{i\omega q}{4\pi^3}\int dt\,\boldsymbol{v}_q e^{i\omega t-i\boldsymbol{kr}_q}\;, \tag{4}$$

$$G(\boldsymbol{k}'-\boldsymbol{k})=\frac{e^2}{2\pi^2 m}\sum_{\alpha}\sum_{\beta=1}^{Z}\delta(\boldsymbol{r}-\boldsymbol{r}_\alpha-\boldsymbol{r}_{\alpha\beta})\,,$$

which describes the scattering and refractive properties of the crystal. Further analysis calls for the separation of the coherent component, describing the refraction effect, from the function $G(\boldsymbol{k}'-\boldsymbol{k})$. Averaging $G(\boldsymbol{k}'-\boldsymbol{k})$ over coordinates of nuclei and electrons, we obtain

$$G(\boldsymbol{k}'-\boldsymbol{k})\equiv\langle G(\boldsymbol{k}'-\boldsymbol{k})\rangle+\widetilde{G}(\boldsymbol{k}'-\boldsymbol{k})\,,\quad \langle G(\boldsymbol{k}'-\boldsymbol{k})\rangle=\omega_0^2\delta(\boldsymbol{k}'-\boldsymbol{k})\,,\quad \omega_0^2=\frac{4\pi Ze^2 n_0}{m}\,, \tag{5}$$

where ω_0 is the plasma frequency of the medium.

Substitution of Eq. (5) into Eq. (4) yields an equation that differs from Eq. (4) as follows:

$$G(\boldsymbol{k}'-\boldsymbol{k})\to\widetilde{G}(\boldsymbol{k}'-\boldsymbol{k})\,,\quad k^2-\omega^2\to k^2-k_0^2\,,\quad k_0^2=\omega^2\left(1-\frac{\omega_0^2}{\omega^2}\right)=\omega^2\varepsilon(\omega)\,. \tag{6}$$

For weak scattering (in the kinematic approximation of diffraction theory), a solution of this equation can be found by iterations

$$\boldsymbol{E}_{k\omega}\approx\frac{i\omega q}{4\pi^3}\frac{1}{k^2-k_0^2}\int dt\,e^{i\omega t}\left\{\left(\boldsymbol{v}_q-\frac{\boldsymbol{k}}{k_0^2}\boldsymbol{k}\boldsymbol{v}_q\right)e^{i\boldsymbol{kr}_q}\right.$$

$$\left.-\int\frac{dk'}{k'^2-k}\widetilde{G}(\boldsymbol{k}'-\boldsymbol{k})\left[\boldsymbol{v}_q-\frac{\boldsymbol{k}'}{k_0^2}\boldsymbol{k}'\boldsymbol{v}_q-\frac{\boldsymbol{k}'}{k_0^2}\left(\boldsymbol{k}\boldsymbol{v}_q-\frac{\boldsymbol{k}\boldsymbol{k}'}{k_0^2}\boldsymbol{k}'\boldsymbol{v}_q\right)\right]e^{-i\boldsymbol{kr}_q}\right\}. \tag{7}$$

It can be easily seen that the first term of Eq. (7), proportional to e^{-ikr_q}, describes the equilibrium electromagnetic field of the fast particle moving in the medium with permittivity ε(ω), and the second term describes scattering of this field on the fluctuations of electron density of the medium.

To find the spectral and angular radiation distribution, the Fourier integral

$$\boldsymbol{E}_\omega(\boldsymbol{r}) = \int d^3k\, \boldsymbol{E}_{\boldsymbol{k}\omega} e^{-i\boldsymbol{kr}}$$

must be calculated. Since we are interested in the radiation field in the wave zone, integration over $d^3\boldsymbol{k}$ can be performed by asymptotic methods:

$$\boldsymbol{E}_\omega(\boldsymbol{r}) = \int d^3k\, \boldsymbol{E}_{\boldsymbol{k}\omega} e^{-i\boldsymbol{kr}} = \boldsymbol{A}_{\boldsymbol{n}} \frac{e^{ik_0 r}}{r}, \tag{8}$$

$$\boldsymbol{A}_{\boldsymbol{n}} = \frac{i\omega q}{2\pi}\int dt\, e^{i\omega t}\left\{(\boldsymbol{v}_q - \boldsymbol{n}\cdot\boldsymbol{n}\boldsymbol{v}_q)e^{ik_0\boldsymbol{n}\boldsymbol{r}_q} - \int \frac{d^3k}{k^2-k_0^2}\tilde{G}(\boldsymbol{k}-k_0\boldsymbol{n})\left[\boldsymbol{v}_q - \frac{\boldsymbol{k}}{k_0^2}\boldsymbol{k}\boldsymbol{v}_q - \boldsymbol{n}\left(\boldsymbol{n}\boldsymbol{v}_q - \frac{\boldsymbol{nk}}{k_0^2}\boldsymbol{k}\boldsymbol{v}_q\right)\right]e^{i\boldsymbol{k}\boldsymbol{r}_q}\right\},$$

where $\boldsymbol{n}$ is the unit vector whose sense coincides with that of radiation emission.

It can be easily seen that for uniform and rectilinear motion of the fast particle, the contribution of the first term of Eq. (8) to the output radiation must vanish. To take the contribution of bremsstrahlung into account, we integrate this term by parts and express the fast-particle acceleration in terms of the crystal potential with the help of the equation of motion. Assuming that the trajectory $\boldsymbol{r}_q(t)$ in the expression for amplitude $\boldsymbol{A}_n$ is rectilinear (in the dipole approximation of radiation theory which holds if the angle of particle scattering in the process of emission is less than γ^{-1} [7]), we find the final expression for the radiation amplitude

$$\boldsymbol{A}_{\boldsymbol{n}} = -iq\int d^3k\left[\frac{1}{k^2}Q(\boldsymbol{k})\boldsymbol{a}_k + \frac{1}{k^2-2k_0\boldsymbol{nk}}\tilde{G}(\boldsymbol{k})\boldsymbol{b}_k\right]\delta\left[\omega\left(1-\sqrt{\varepsilon}\boldsymbol{nv}\right)-\boldsymbol{kv}\right], \tag{9}$$

$$Q(\boldsymbol{k}) = \frac{eq}{2\pi^2 m}\sum_\alpha e^{i\boldsymbol{k}\boldsymbol{r}_\alpha}\left(Z - \sum_{\beta=1}^{Z} e^{i\boldsymbol{k}\boldsymbol{r}_{\alpha\beta}}\right),$$

$$\boldsymbol{a}_k = \frac{\boldsymbol{k}-\boldsymbol{v}\boldsymbol{kv}}{1-\sqrt{\varepsilon}\boldsymbol{v}} - \frac{\boldsymbol{n}-\sqrt{\varepsilon}\boldsymbol{v}}{(1-\sqrt{\varepsilon}\boldsymbol{nv})^2}(\boldsymbol{nk}-\boldsymbol{nv}\boldsymbol{kv}),$$

$$\tilde{G}(\boldsymbol{k}) = \frac{e^2}{2\pi^2 m}\sum_\alpha\sum_{\beta=1}^{Z} e^{i\boldsymbol{k}(\boldsymbol{r}_\alpha+\boldsymbol{r}_{\alpha\beta})} - \omega_0^2\delta(\boldsymbol{k}),$$

$$\boldsymbol{b}_k = \boldsymbol{v}\frac{\boldsymbol{kv}}{1-\sqrt{\varepsilon}\boldsymbol{nv}} - \boldsymbol{k}\frac{1}{\varepsilon} - \boldsymbol{n}\left(\boldsymbol{nv}\frac{\boldsymbol{kv}}{1-\sqrt{\varepsilon}\boldsymbol{nv}} - \boldsymbol{nk}\frac{1}{\varepsilon}\right).$$

We note that in the derivation of Eq. (9) we did not use any additional assumptions on the structure of the substance. Therefore, formula (9) can be used to investigate the properties of radiation emitted by the fast electron in a medium with arbitrary structure.

The term of Eq. (9) proportional to $Q(\boldsymbol{k})$ corresponds to the bremsstrahlung (BS) of the fast particle interacting with atomic nuclei and electrons of the medium, and the term proportional to $\hat{G}(k)$ describes the polarization bremsstrahlung (PBS) of the particle interacting with atomic electrons [8]. Before we proceed to an analysis of the spectral and angular radiation characteristics, we note that amplitude (9) correctly describes the interference effect in the nonrelativistic limit ($v << 1$) [9] when the PBS and BS are mutually destroyed on the electrons when the radiating particle is a nonrelativistic electron. Indeed, from Eq. (9) it follows that $\boldsymbol{a}_k \approx -\boldsymbol{b}_k \approx \boldsymbol{k} - \boldsymbol{n}\cdot\boldsymbol{nk}$ ($\varepsilon \approx 1$) and $k^2 + 2\omega\sqrt{\varepsilon}\boldsymbol{nk} \approx k^2$ for $v << 1$; therefore, the electron contributions to the BS and PBS are cancelled for $q = -e$ ($\varepsilon > 0$). As a result, the net radiation is reduced only to the bremsstrahlung of the nonrelativistic electron on the nuclei [9].

2. SPECTRAL AND ANGULAR RADIATION DISTRIBUTION

The expression for the spectral and angular distribution of the number of emitted photons, which follows from Eq. (9), has the form

$$\omega\frac{d^2N}{d\omega\, dO} = \left\langle |A_n|^2 \right\rangle = \sum_{j=1}^{3}\omega\frac{d^2N^{(j)}}{d\omega\, dO}, \tag{10}$$

where the first term corresponds to the BS, the second term characterizes the PBS, and the third term describes the interference between the BS and PBS amplitudes. Let us consider first the BS characteristics

$$\omega\frac{d^2N^1}{d\omega\, dO} = \omega\frac{d^2N^{\mathrm{br}}}{d\omega\, dO} = q^2\int\frac{d^3k}{k^2}\frac{d^3k'}{k'^2}\langle Q(\boldsymbol{k})Q^*(\boldsymbol{k}')\rangle \boldsymbol{a}_k\boldsymbol{a}_{k'}\delta\big(\omega(1-\sqrt{\varepsilon}\boldsymbol{nv})-\boldsymbol{kv}\big)\delta\big(\omega(1-\sqrt{\varepsilon}\boldsymbol{nv})-\boldsymbol{k}'\boldsymbol{v}\big). \tag{11}$$

Here the angular brackets denote averaging over random variables $\boldsymbol{r}_\alpha$ and $\boldsymbol{r}_{\alpha\beta}$. In the examined case of the crystal medium, $\boldsymbol{r}_{\alpha\square} = \boldsymbol{r}_n + \boldsymbol{r}_{nl} + \boldsymbol{u}_{nl}$, where $\boldsymbol{r}_n$ are coordinates of the nth elementary crystal cell, $\boldsymbol{r}_{nl}$ is the equilibrium position of the lth atom in the nth cell, and $\boldsymbol{u}_{nl}$ is the thermal displacement of the atom. After averaging over the thermal displacements $\boldsymbol{u}_{nl}$, we obtain the conventional Debye–Waller factor. Averaging over electron coordinates $\boldsymbol{r}_{nl\beta}$, we perform for the statistical atomic model with exponential screening. The result of averaging has the form

$$\langle Q(\boldsymbol{k})Q^*(\boldsymbol{k}')\rangle = \frac{2e^4 n_0}{\pi m^2\gamma^2}\left\{Z^2\frac{k^4R^4}{(1+k^2R^2)^2}\left[(2\pi)^3 n_0 |S(\boldsymbol{k})|^2 e^{-k^2u^2}\sum_{\boldsymbol{g}}\delta(\boldsymbol{k}-\boldsymbol{g}) + 1 - e^{-k^2u^2}\right]\right.$$

$$\left. + Z\left(1 - \frac{1}{(1+k^2R^2)^2}\right)\right\}\delta(\boldsymbol{k}-\boldsymbol{k}') \equiv \frac{2e^4 n_0}{\pi m^2\gamma^2}F^{\mathrm{br}}(\boldsymbol{k})\delta(\boldsymbol{k}-\boldsymbol{k}'), \tag{12}$$

where R is the screening radius of the statistical atomic model,

$$S(\boldsymbol{k}) = \frac{1}{N}\sum_{l=1}^{N} e^{i\boldsymbol{k}\boldsymbol{r}_{nl}},$$

N is the number of atoms in the elementary cell of volume Ω, $n_0 = N/\Omega$, u is the rms amplitude of thermal atomic displacement, and $\boldsymbol{g}$ is the vector of the reciprocal crystal lattice.

Terms of Eq. (12) containing δ-functions $\delta(\boldsymbol{k}-\boldsymbol{g})$ correspond to the coherent bremsstrahlung of the fast particle in the crystal. The next term proportional to $(1 - e^{-k^2u^2})$ corresponds to the incoherent bremsstrahlung of the screened crystal atoms. The term of Eq. (12) proportional to the number of electrons in the atom Z corresponds to the individual electron contributions to the bremsstrahlung (the Landau–Rumer correction factor) [10].

Substitution of Eq. (12) into general formula (11) yields the following expression for the spectral and angular distribution of the BS intensity:

$$\omega\frac{d^3N^{\rm br}}{dt\,d\omega dO}=\frac{e^6 n_0}{\pi^2 m^2\gamma^2(1-\sqrt{\varepsilon}\boldsymbol{nv})^2}\int\frac{d^3k}{k^4}\left[\boldsymbol{k}-\boldsymbol{vkv}-\frac{\boldsymbol{n}}{1-\sqrt{\varepsilon}\boldsymbol{nv}}(\boldsymbol{nk}-\boldsymbol{nvkv}\right]^2 F^{\rm br}(\boldsymbol{k})\delta\left[\omega(1-\sqrt{\varepsilon}\boldsymbol{nv})-\boldsymbol{kv}\right]. \quad (13)$$

Similar calculations yield the following formula for the PBS intensity distribution:

$$\omega\frac{d^3N^2}{dt\;d\omega\,dO}\equiv\omega\frac{d^3N^{\rm pb}}{dt\;d\omega\,dO}=\frac{e^6 n_0}{\pi^2 m^2}\int\frac{d^3k'}{(k^2+2\omega\sqrt{\varepsilon}\boldsymbol{nk})^2}\left[\boldsymbol{v}\omega-\boldsymbol{k}\frac{1}{\varepsilon}-\boldsymbol{n}\left(\boldsymbol{nv}\omega-\boldsymbol{nk}\frac{1}{\varepsilon}\right)\right]^2 F^{\rm br}(\boldsymbol{k})\delta\left[\omega(1-\sqrt{\varepsilon}\boldsymbol{nv})-\boldsymbol{kv}\right], \quad (14)$$

$$F^{\rm br}(\boldsymbol{k})=\frac{Z^2}{(1+k^2R^2)^2}\left[(2\pi)^3 n_0\left|S(\boldsymbol{k})\right|^2 e^{-k^2u^2}\sum_{\boldsymbol{g}}\delta(\boldsymbol{k}-\boldsymbol{g})+1-e^{-k^2u^2}\right]+Z\left[1-\frac{1}{(1+k^2R^2)^2}\right].$$

The interference term in Eq. (10) is proportional to the sign of the fast-particle charge

$$\omega\frac{d^3N^3}{dt\;d\omega\,dO}\equiv\omega\frac{d^3N^{\rm int}}{dt\;d\omega\,dO}={\rm sign}(q)\frac{e^6 n_0}{\pi^2 m^2\gamma(1-\sqrt{\varepsilon}\boldsymbol{nv})}\int\frac{d^3k}{k^2(k^2+2\omega\sqrt{\varepsilon}\boldsymbol{nk})}\left[\boldsymbol{v}\omega-\boldsymbol{k}\frac{1}{\varepsilon}-\boldsymbol{n}\left(\boldsymbol{nv}\omega-\boldsymbol{nk}\frac{1}{\varepsilon}\right)\right]$$

$$\times\left[\boldsymbol{k}-\boldsymbol{vkv}-\frac{\boldsymbol{n}-\sqrt{\varepsilon}\boldsymbol{v}}{1-\sqrt{\varepsilon}\boldsymbol{nv}}\left(\boldsymbol{nk}-\boldsymbol{nvkv}\right)\right]F^{\rm int}(\boldsymbol{k})\delta\left[\omega(1-\sqrt{\varepsilon}\boldsymbol{nv})-\boldsymbol{kv}\right]. \quad (15)$$

Proceeding to an analysis of the formulas obtained, we indicate some general properties of the examined radiation.

First we note [11] that the PBS component in formula (14) coherent throughout the crystal is analogous to the well-known PXR [1–3] considered usually within the framework of the macroscopic approach [12–14].

A comparison of BS and PBS components, incoherent throughout the crystal but coherent for the atomic electrons, demonstrates sharply different effects of thermal oscillations of the crystal atoms on the above-indicated emission mechanisms. From the expression for $F^{\rm br}(\boldsymbol{k})$ it follows that the main contribution to the BS comes from large momenta $k > R^{-1}$, that is, small impact parameters upon collision of a fast particle with an atom $b < R^{-1}$ (the contribution of collisions with $b >> R^{-1}$ is cancelled due to screening of the nucleus by the atomic electrons). On the other hand, the expression for $F^{\rm br}(\boldsymbol{k})$ demonstrates that the output PBS is largely determined by collisions with impact parameters $b > R^{-1}$ (the contribution of collisions with $b < R^{-1}$ to the PBS component coherent for the atomic electrons is cancelled, since in this case parts of the electronic "fur-coat" of the atom arranged on the opposite sides of the fast particle trajectory are displaced in diametrically opposite directions, thereby leading to a decrease in the coherent current induced by the atomic electrons and responsible for the PBS). Due to the above-indicated reasons, the factor $(1-e^{-k^2u^2})$, which enters into the cross sections of the incoherent BS and PBS, will be close to unity for the BS and small for the PBS. Thus, the incoherent PBS component in the crystal, unlike the incoherent BS component, will be sharply suppressed [15].

The fact that individual electron contributions to the BS and PBS cross sections and to the interference term have opposite signs has engaged our attention. To explain this effect, we note that the examined factor entering into the interference term of Eq. (15) is proportional to the average product of the alternating current caused by scattering of the fast particle on the electrons of the medium by the electron current of the medium induced by the particle. Obviously, these currents have opposite directions, thereby leading to the minus sign in the formula for $F^{\rm int}(\boldsymbol{k})$. On the other hand, products of quantities of common physical nature are averaged in correlators $\langle Q(\boldsymbol{k})Q^*(\boldsymbol{k}')\rangle$ and $\langle G(\boldsymbol{k})G^*(\boldsymbol{k}')\rangle$, thereby giving the plus sign of the corresponding terms of formulas (12) and (14).

In the present work, we restrict ourselves to an analysis of the radiation component coherent throughout the crystal and caused by scattering of the fast particle and its field on a system of parallel atomic planes of the crystal specified by the reciprocal lattice vector $\boldsymbol{g}$. The general expression for the total coherent radiation follows from expressions (12)–(15) and has the form

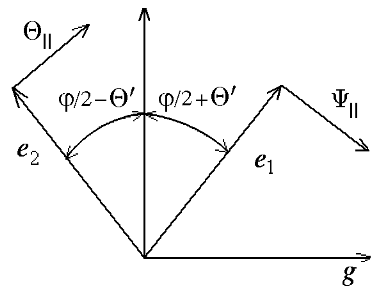

Fig. 1. Angular variables of the examined problem.

$$\omega\frac{d^3N_g}{dt\,d\omega\,dO}=\frac{8\pi Z^2e^6n_0^2|S(\boldsymbol{g})|^2e^{-g^2u^2}}{m^2(1+g^2R^2)^2}\left\{\mathrm{sign}(q)\frac{R}{\gamma(1-\sqrt{\varepsilon}\boldsymbol{nv})}\left[\boldsymbol{g}-\boldsymbol{vgv}-\frac{\boldsymbol{n}\sqrt{\varepsilon}\boldsymbol{v}}{1-\sqrt{\varepsilon}\boldsymbol{nv}}(\boldsymbol{ng}-\boldsymbol{nvgv})\right]+\frac{1}{f^2+2\omega\sqrt{\varepsilon}\boldsymbol{ng}}\right.$$

$$\left.\times\left[\boldsymbol{v}\omega-\boldsymbol{g}\frac{1}{\varepsilon}-\boldsymbol{n}\left(\boldsymbol{nv}\omega-\boldsymbol{ng}\frac{1}{\varepsilon}\right)\right]\right\}\delta\left(\omega(1-\sqrt{\varepsilon}\boldsymbol{nv})-\boldsymbol{gv}\right), \tag{16}$$

explicitly indicating an interference between the coherent BS and PBS components.

For further analysis, it is convenient to introduce two-dimensional variables Ψ and Θ to describe the angular width of the beam of fast particles and the angular distribution of the emitted photons, respectively. We assume

$$\begin{aligned}\boldsymbol{v}&=\boldsymbol{e}_1\left(1-\frac{\gamma^2}{2}\frac{\Psi^2}{4}\right)\Psi, \quad \Psi\boldsymbol{e}_1=0,\\ \boldsymbol{n}&=\boldsymbol{e}_2\left(1-\frac{\Theta^2}{2}\right)+\Theta, \quad \boldsymbol{e}_2\Theta=0,\end{aligned} \tag{17}$$

where the unit vector $\boldsymbol{e}_1$ is directed along the beam axis of radiating particles and the vector $\boldsymbol{e}_2$ is directed along the axis of the radiation detector. In our experimental design, the vectors $\boldsymbol{e}_1$and $\boldsymbol{e}_2$ remain fixed; as a rule, $\boldsymbol{e}_1\boldsymbol{e}_2=\cos\varphi$, $\varphi=\mathrm{const}$; however, the crystal target is rotated about the beam of particles with the help of a goniometer (thereby changing the sense of the reciprocal lattice vector $\boldsymbol{g}$). In the experiment, vectors $\boldsymbol{g}$, $\boldsymbol{e}_1$, and $\boldsymbol{e}_2$ lie in one plane. Of primary interest is the dependence of the emitted energy distribution (or of the number of photons) on the orientation angle of the velocity vector of the fast particle with the reflecting crystallographic plane. In the examined problem, the orientation dependence is described by the angle Θ' counted off from the reflecting plane corresponding to the exact condition of Bragg's resonance (see Fig. 1 which also shows the directions of changing components $\Psi_{\|}$ and $\Theta_{\|}$; the components $\Psi_{\perp}$ and $\Theta_{\perp}$ change in the plane perpendicular to that of the figure).

In the examined case of small angles $\varphi \ll 1$, the substitution of Eqs. (17) into general formula (16) yields the following expression:

$$\omega\frac{d^4N_g}{dt\,d\omega\,d^2\Theta}=W_g\frac{F^2}{\Omega_1}\delta\left[\omega-g\frac{\varphi+2\Theta'+2\Theta_{\|}}{\Omega_1}\right], \tag{18}$$

where

$$W_g = \frac{16\pi Z^2 e^6 n_0^2}{m^2 g^2} \frac{|S(\boldsymbol{g})|^2 e^{-g^2 u^2}}{1 + g^2 R^2},$$

$$\boldsymbol{F} = \frac{2g^2 R^2}{\gamma} \frac{1}{\Omega_1^2} \left\{ \boldsymbol{e}_z 2(\Theta_\perp - \Psi_\perp)(\varphi - \Theta_\parallel + \Psi_\parallel) + \boldsymbol{e}_x \left[\gamma^{-2} + \frac{\omega_0^2}{\omega^2} + (\Theta_\perp - \Psi_\perp)^2 - (\varphi - \Theta_\parallel + \Psi_\parallel)^2 \right] \right\} \mathrm{sign}\,(q)$$

$$- \frac{1}{\Omega_2} \left\{ \boldsymbol{e}_z 2(\Theta_\perp - \Psi_\perp)(\varphi + 2\Theta' + 2\Psi_\parallel) + \boldsymbol{e}_x \left[\gamma^{-2} + \frac{\omega_0^2}{\omega^2} + (\Theta_\perp - \Psi_\perp)^2 - (2\Theta' + \Theta_\parallel)(\varphi - \Theta_\parallel + \Psi_\parallel) \right] \right\},$$

$$\Omega_1 = \gamma^{-2} + \frac{\omega_0^2}{\omega^2} + (\Theta_\perp - \Psi_\perp)^2 - (\varphi - \Theta_\parallel + \Psi_\parallel)^2,$$

$$\Omega_2 = \gamma^{-2} + \frac{\omega_0^2}{\omega^2} + (\Theta_\perp - \Psi_\perp)^2 - (2\Theta' + \Theta_\parallel + \Psi_\parallel)^2.$$

Below we analyze the radiation properties based on these expressions.

3. INFLUENCE OF INTERFERENCE ON THE ORIENTATION DEPENDENCE OF THE OUTPUT RADIATION

Proceeding to an analysis of Eq. (18), we note first some characteristic features of radiation that are manifested exactly in the examined case of small orientation angles of the radiating particle velocity with the crystallographic plane. According to the argument of the δ-function in Eq. (18), the energy of photon emitted in the direction of the observation angle Θ depends on both components $\Theta_\perp$ and $\Theta_\parallel$ of the observation angle and on the parameter Ψ specifying the angular beam width of radiating particles. In other words, the emission spectrum broadens significantly due to multiple scattering of radiating particles and finite angular aperture of the collimator. However, for sufficiently large angles φ

$$1 >> \varphi >> \gamma^{-1},\ \Theta,\ \Psi,\ \Theta',\ \frac{\omega_0}{\omega} \tag{19}$$

the argument of the δ-function in Eq. (18) assumes the form

$$\omega - g \frac{\varphi + 2\Theta' + 2\Psi_\parallel}{\gamma^{-2} + \omega_0^2/\omega^2 + (\Theta_\perp - \Psi_\perp)^2 - (\omega - \Theta_\parallel + \Psi_\parallel)^2} \approx \omega - \omega_B \left(1 + 2 \frac{\Theta' + \Theta_\parallel}{\varphi} \right), \tag{20}$$

where $\omega_B = g/\varphi$ is Bragg's frequency. From Eq. (20) it follows that for angles φ satisfying inequality (19), multiple scattering has no effect on the energy of photons propagating at the given angle. Moreover, the difference between the photon and Bragg's energy is determined only by the orientation angle Θ′ and one component of the observation angle $\Theta_\parallel$.

We also note a significant difference between the angular distributions of bremsstrahlung and parametric radiation components which follows from Eq. (18) after integration over ω. It can be easily seen that for $\varphi \approx \gamma^{-1}$, the number of bremsstrahlung photons emitted per unit time

$$\frac{d^3 N}{dt\, d^2\Theta} = \int d\omega \frac{d^4 N}{dt\, d\omega\, d^2\Theta}$$

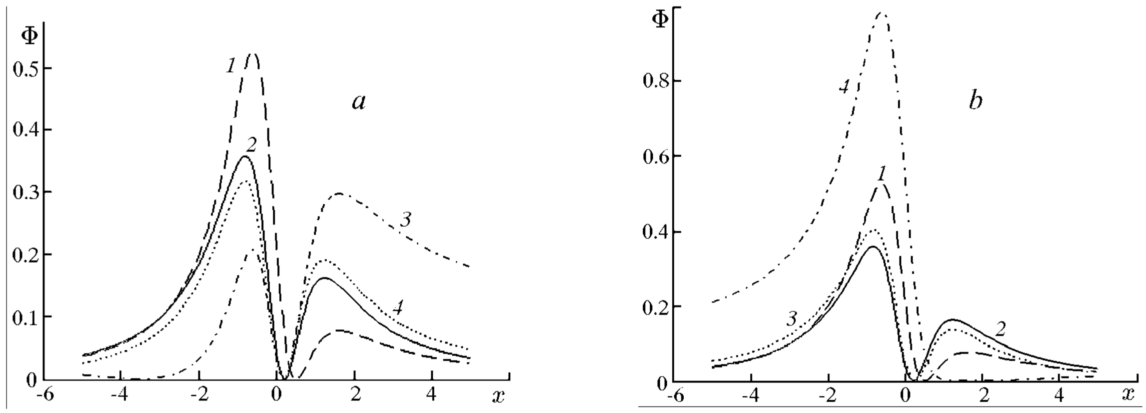

Fig. 2. Orientation dependence of the output radiation for the electrons (*a*) at α = 0 (*1* and *2*) and 5 (*3* and *4*) and β = 2 (*1* and *3*) and 5 (*2* and *4*) and for the positrons (*b*) at α = 0 (*1* and *2*), 2 (*4*), and 5 (*3*) and β = 2 (*1* and *4*) and 5 (*2* and *3*).

decreases as Θ^{-4} for $\Theta >> \gamma^{-1}$, and the angular distribution of the bremsstrahlung intensity

$$\frac{d^3E}{dt\, d^2\Theta} = \int d\omega\, \omega \frac{d^4E}{dt\, d\omega\, d^2\Theta}$$

decreases more rapidly, as Θ^{-6}. On the other hand, the number of PXR photons in the examined conditions does not decrease with increasing Θ, and the PXR intensity is of the order of Θ^{-2}. Thus, to calculate the angular distribution of the number of PXR photons for small radiation angles $\varphi \approx \gamma^{-1}$, we cannot use the expansions that were used in the derivation of Eq. (18).

For large angles $\varphi >> \gamma^{-1}$, the situation sharply changes. It can be easily seen that the angular distribution of the coherent bremsstrahlung component at $\Theta << \varphi$ becomes uniform and the PXR angular distribution is narrowed markedly:

$$\frac{d^3N}{dt\, d^2\Theta} \propto \Theta^{-2}, \quad \frac{d^3E}{dt\, d^2\Theta} \propto \Theta^{-4} \quad \text{for} \quad \Theta >> \gamma^{-1}.$$

To analyze the orientation dependence of the output collimated radiation (the angular aperture of the collimator $\Theta_d < \gamma^{-1}$ and the plane of the photon detector coincides with the plane $\Theta_\perp = 0$), we take advantage of Eq. (18). The radiation intensity is determined by the formula

$$\frac{dE_g}{dt} = \pi\gamma^2\Theta_d^2 W_g \Phi(x, \alpha, \beta), \tag{21}$$

where

$$\Phi = \frac{1}{\beta^2+1}\left[\alpha \frac{\beta^2-1}{(\beta^2+1)^2}\,\mathrm{sign}\,(q) + \frac{1-x\beta}{1+x^2}\right],$$

$x = 2\gamma\Theta'$, $\alpha = 2\gamma g^2 R^2$, and $\beta = \gamma\varphi$. In the derivation of Eq. (21) we have neglected the influence of multiple scattering and considered that the condition $\gamma^2\omega^2 << \omega_B^2$ employed for the PXR component is satisfied within the framework of the kinematic approach. Figure 2 shows the dependences $\Phi(x)$ drawn by formula (21) for the electrons ($q = -|e|$) and positrons

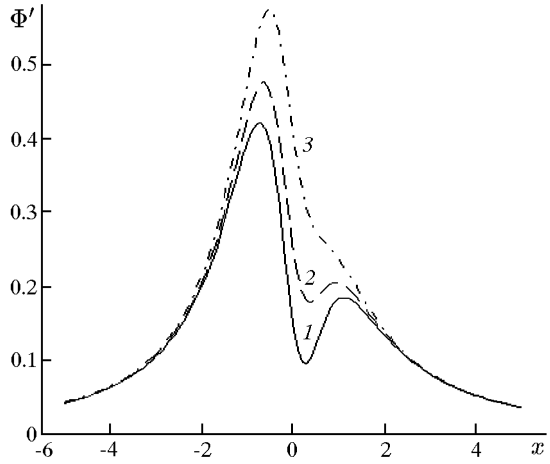

Fig. 3. Effect of multiple scattering on the orientation dependence of electrons. The curves are drawn for the following fixed values of the parameters: $\gamma^2\Psi_0^2 = 0.05$, $\alpha = 0$, and $\beta = 5$ and for $\gamma^2\Psi_s^2 T = 0.1$ (1), 0.3 (2), and 0.6 (3).

($q = |e|$) as functions of the parameters α and β. The curves in the figure demonstrate the sharp difference in the interference effects for positrons and electrons increasing with decreasing parameter $\gamma\varphi$.

Formula (18) is convenient for analyzing the influence of multiple scattering of the radiating particles on the emitted photon characteristics. Approximating the distribution function of the beam electrons by the simple dependence

$$f(t,\Psi) = \frac{1}{\pi(\Psi^2 + \Psi t)} \exp\left(-\frac{\Psi^2}{\Psi_0^2 + \Psi_s^2 t}\right), \tag{22}$$

where Ψ_0 is the initial beam divergence,

$$\Psi_s^2 = \frac{\varepsilon_k^2}{m^2\gamma^2}\frac{1}{L_R}$$

is the mean-square multiple scattering intensity per unit of length, $\varepsilon_k \approx 21$ MeV, and L_R is the radiation length, from Eq. (18) we obtain

$$\frac{1}{T}\langle E_g\rangle = \frac{1}{T}\int_0^T dt \int d^2\Psi\, f(t,\Psi) \int d^2\Theta \int d\omega\, \omega \frac{d^4 N_g}{dt\, d\omega\, d^2\Theta} = \pi\gamma^2\Theta_d^2 W_g \Phi'(x,\alpha,\beta,\gamma^2\Psi_0^2,\gamma^2\Psi_s^2 T). \tag{23}$$

Figure 3 shows the function $\Phi'(x)$ specified by Eq. (21). The curves of orientation dependence of the radiation intensity drawn by Eq. (23) for fixed values of the parameters α, β, and $\gamma^2\Psi_0^2$ as functions of the parameter $\gamma^2\Psi_s^2 T$, equal to the ratio of the mean-square intensity multiply scattered on the crystal thickness T to the square of the characteristic angle of the relativistic particle emission, demonstrate significant distortion of the examined dependence with increasing crystal thickness.

4. INFLUENCE OF INTERFERENCE ON THE POLARIZATION RADIATION CHARACTERISTICS

We now analyze the polarization of emitted photons under conditions of interference between the bremsstrahlung and parametric radiation. According to general expression (18), the direction of the electric field vector of the emitted wave

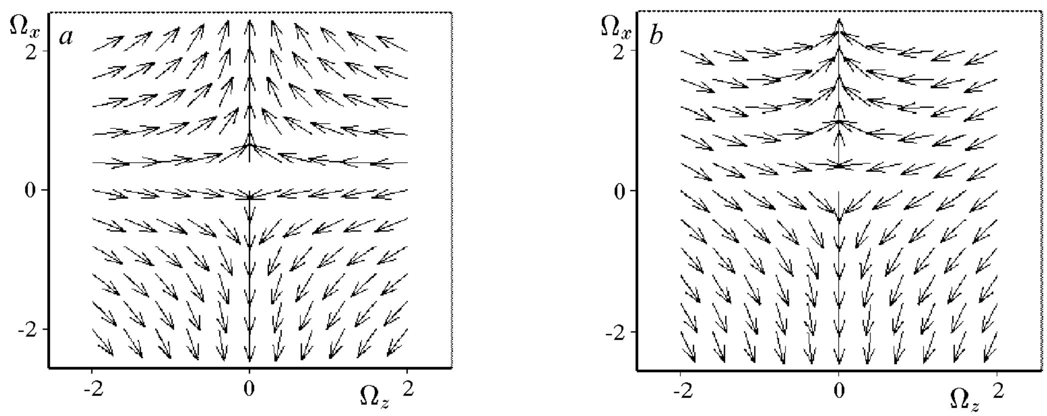

Fig. 4. Vector field of polarization of the parametric radiation for the observation angle β = 10 (*a*) and 3 (*b*).

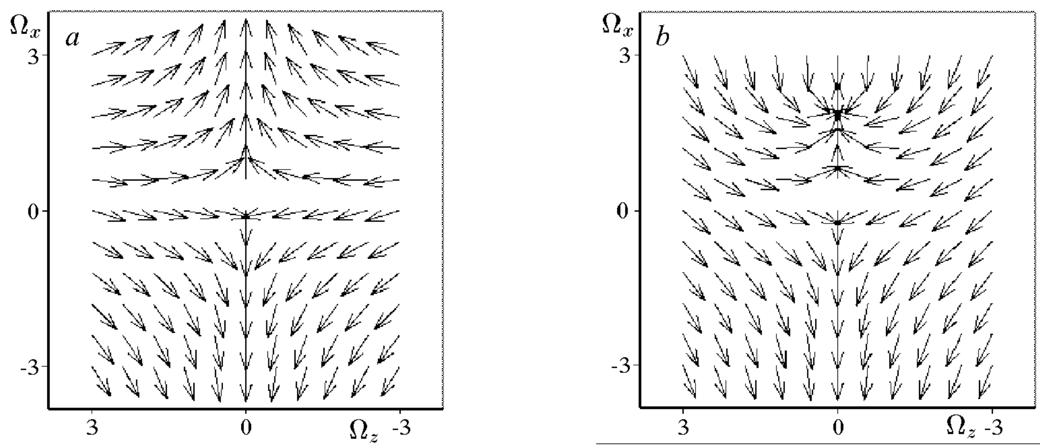

Fig. 5. Influence of the interference effect on the polarization of electron radiation for α = 5 and β = 10 (*a*) and 3 (*b*).

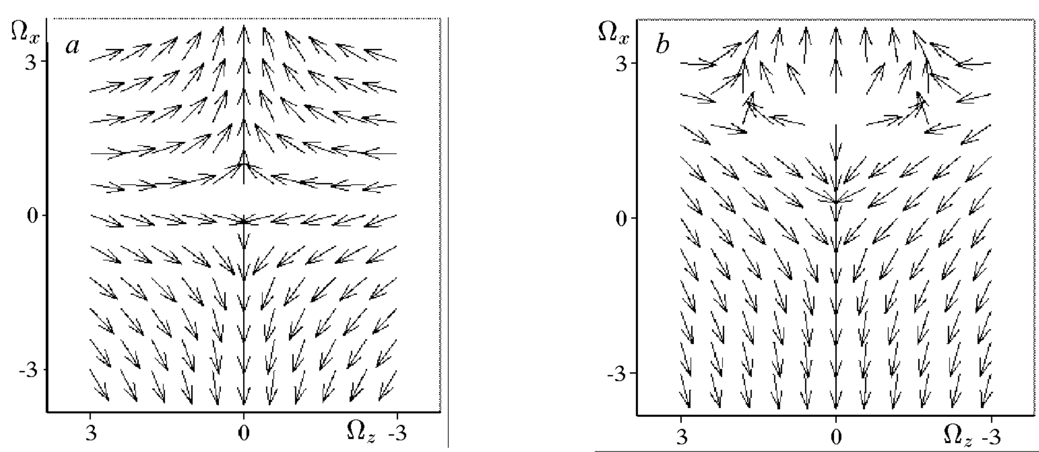

Fig. 6. Influence of the interference effect on the polarization of positron radiation for α = 5 and β = 10 (*a*) and 3 (*b*).

is determined by vector $\boldsymbol{F}$. Neglecting the effect of multiple scattering, we consider the angular dependence of polarization for exact Bragg's resonance $\Theta' = 0$. The polarization state is described by the unit vector

$$\boldsymbol{f} = \frac{\boldsymbol{F}}{F},$$

$$\boldsymbol{F} = \boldsymbol{e}_z \left[\frac{2\alpha(\beta - \Omega_x)}{(1+\beta^2 + \Omega_x^2 + \Omega_z^2 - 2\beta\Omega_x)^2} \operatorname{sign}(q) - \frac{\beta}{1+\Omega_x^2 + \Omega_z^2} \right] \Omega_z$$

$$+ \boldsymbol{e}_x \left[\frac{\alpha(1-\beta^2 + \Omega_z^2 - \Omega_x + 2\beta\Omega_x)}{(1+\beta^2 + \Omega_x^2 + \Omega_z^2 - 2\beta\Omega_x)^2} \operatorname{sign}(q) - \frac{1+\Omega_x^2 + \Omega_z^2 - \beta\Omega_x}{1+\Omega_x^2 + \Omega_z^2} \right], \quad (24)$$

where $\Omega_x = \gamma\Theta_{\|}$, $\Omega_z = \gamma\Theta_{\perp}$, and the remaining notation coincides with that introduced above.

First we examine the vector field of PXR polarization disregarding its interference with the coherent bremsstrahlung. According to Eq. (24), this case is realized for $\alpha \ll 1$ or $\beta \gg 1$ and is of independent interest in connection with the continuing discussion about the character of the vector field of PXR polarization when the fast particle is incident on the reflecting crystallographic plane at angles $\varphi/2 \leq \pi/4$. In the examined case, the convenient formula

$$\boldsymbol{f}^{\mathrm{PXR}} = \frac{\boldsymbol{e}_z\beta\Omega_z + \boldsymbol{e}_x(1+\Omega_x^2 + \Omega_z^2 - \beta\Omega_x)}{\sqrt{\beta^2\Omega_z^2 + (1+\Omega_x^2 + \Omega_z^2 - \beta\Omega_x)^2}} \quad (25)$$

follows from Eq. (24).

It can be easily seen that for large orientation angles $\varphi \gg \gamma^{-1}$, Eq. (25) confirms the viewpoint of [16] (in this case, $f^{\mathrm{PXR}} \gg (e_z\Omega_z - e_x\Omega_x)/\sqrt{\Omega_z^2 + \Omega_x^2}$); however, distribution (25) changes significantly as the parameter β decreases. Figure 4 shows vector field (25) for the indicated values of the parameter β.

The structure of vector field (24) changes especially significantly when the interference effect is manifested. In this case, the character of the polarization vector field depends not only on the angle φ but also on the parameter α, which characterizes the relative contribution of the coherent bremsstrahlung, and on the sign of the emitting particle charge. Figures 5 and 6 show the angular distributions of polarization of electron and positron radiation, respectively, which demonstrate the sharp change of the character of photon polarization with increasing degree of overlap between the propagation cones of PXR radiation and coherent bremsstrahlung as the orientation angle φ decreases.

5. EXPERIMENTAL FACILITY FOR INVESTIGATION OF THE PARAMETRIC RADIATION AND COHERENT BREAMSSTRAHLUNG OF RELATIVISTIC ELECTRONS IN A CRYSTAL

We plan to investigate the salient features of the orientation and polarization characteristics of coherent x rays emitted by relativistic particles in a crystal, which have been established in the present work, using a microtron developed at the Institute of Physics of the Russian Academy of Sciences (IPRAS). Figure 7 shows the block diagram of the experimental facility. A microtron with an energy 7 MeV serves as the injector for the Pakra accelerator. An electron beam is extracted from the injection channel with magnet M1 and is narrowed by collimators K1 and K2 to a diameter of several millimeters. Then the beam is deflected by magnet M2 and is focused by lenses L1 and L2 on a crystalline target placed in goniometer G which has two orientation axes changeable with a step of 50 μrad and a rotation axis of the target about the azimuth with a step of 1°. Magnet M3, placed behind the target, serves to direct the beam into an absorbent. X rays are recorded with a silicon-filled detector with electric resolution of the order of 200 eV. The radiation polarization is measured

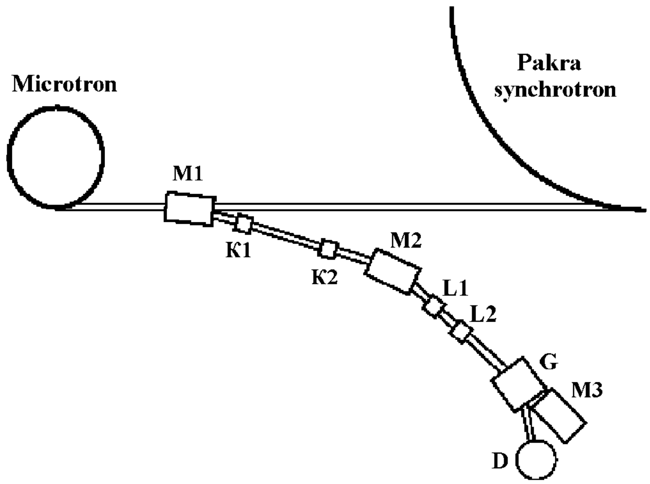

Fig. 7. Block diagram of the experimental facility.

by a Compton polarimeter built around a crystal diffractometer. The facility is equipped with a beam diagnostic system and is remotely controlled.

A silicon crystal 30 μm in thickness is used as the target. In our experiment, the reflecting crystallographic plane is the (220) one. On the one hand, this plane is one of the most closely packed, thereby ensuring efficient scattering of the electromagnetic field of relativistic electron, and on the other hand, large absolute value of the reciprocal lattice vector $\boldsymbol{g}$, corresponding to this plane, will allow us to obtain significant interference between the parametric radiation and the coherent bremsstrahlung (the interference term in the radiation cross section is proportional to the coefficient $\alpha = 2\gamma g^2 R^2$).

The choice of the observation angle φ in the experiment is dictated by two basic reasons: first of all, the interference effect must be significant and hence the coefficient $\beta = \gamma\varphi$, according to theoretical predictions, must be about several units; on the other hand, Bragg's frequency $\omega_B = g/\varphi$, in the vicinity of which the radiation is concentrated, should fall within the 10–30 keV working range of the radiation detector. The electron energy in the experiment is $m\gamma = 6$ MeV; therefore, the selected observation angle $\varphi = 18°$ will allow us to obtain significant interference effect ($\beta = 4$) and Bragg's frequency $\omega_B \approx 20$ keV convenient for spectrometric and polarization measurements.

CONCLUSIONS

Based on the results of our theoretical analysis of x-ray emission by relativistic charged particles moving at a small angle to the crystallographic plane, we conclude that:

– Efficient interference between the coherent bremsstrahlung and parametric radiation is manifested under the examined conditions, which depends on the sign of the radiating particle charge.

– The interference causes significant spectral and angular redistribution of radiation which may be accompanied by a significant increase in the radiation brightness.

– The interference changes dramatically the angular dependence of polarization of the radiation.

– The examined interference effect takes place for photon energies convenient for experimental realization with the use of the facility built around the 7-MeV microtron developed at the IPRAS and allowing us to measure the spectral, angular, and polarization characteristics of radiation.

This work was supported in part by the Russian Fund for Fundamental Researches (Grants Nos. 99-02-18183 and 00-02-16388).

REFERENCES

1. M. L. Ter-Mikaelian, High-Energy Electromagnetic Processes in Condensed Media, Wiley Interscience, New York (1972).
2. V. G. Baryshevskii and I. D. Feranchuk, Zh. Eksp. Teor. Fiz., **61**, 944 (1971).
3. G. M. Garibyan and C. Yang, Zh. Eksp. Teor. Fiz., **61**, 930 (1971).
4. V. L. Kleiner, N. N. Nasonov, and A. G. Safronov, Phys. Status Solidi, **B181**, 223 (1994).
5. S. V. Blazhevich, G. I. Bochek, V. I. Kulibaba, *et al.*, Phys. Lett., **A195**, 210 (1994).
6. Z. G. Pinsker, Dynamic X-ray Scattering in Ideal Crystals [in Russian], Nauka, Moscow (1974).
7. L. D. Landau and E. M. Lifshits, Field Theory [in Russian], Nauka, Moscow (1973).
8. M. Amus'ia, V. Buimistrov, B. Zon, *et al.* Polarization Bremsstrahlung of Particles and Atoms, Plenum Press, N.Y. (1992).
9. V. M. Buimistrov and L. I. Trakhtenberg, Zh. Eksp. Teor. Fiz., **69**, 108 (1975).
10. L. Landau and G. Rumer, Proc. Roy. Soc., **166**, 213 (1938).
11. V. L. Lapko and N. N. Nasonov, Zh. Tekh. Fiz., **55**, 160 (1990).
12. V. G. Baryshevsky and I. D. Feranchuk, J. Phys. (Paris), **44**, 913 (1983).
13. G. M. Garibian and C. Yang, Nucl. Instrum. Methods, **A248**, 29 (1986).
14. A. Caticha, Phys. Rev., **B45**, 9541 (1992).
15. N. N. Nasonov and A. G. Safronov, in: Proc. Int. Symp. RREPS-93, Tomsk (1993).
16. K. H. Schmidt, G. Buschhorn, R. Kotthaus, *et al.*, Nucl. Instrum. Methods, **B145**, 8 (1998).